Measurement of the Lamb Shift in Hydrogen, $n=2$

S. R. Lundeen and F. M. Pipkin
Lyman Laboratory of Physics, Harvard University, Cambridge, Massachusetts 02138
(Received 7 August 1980)

A measurement based on the fast–atomic-beam separated–oscillatory-field method of sub-natural-linewidth spectroscopy gives, for the Lamb shift in hydrogen, $\mathcal{S}(n=2) = 1057.845(9)$ MHz. The result is not in good agreement with theory.

PACS numbers: 35.10.Fk, 32.70.Jz

The most precise tests of radiative corrections to electromagnetic interactions are the electron's anomalous magnetic moment and the Lamb shift in hydrogen. In spite of the long history of refinement of both of these tests, neither can now be said to agree satisfactorily with the predictions of QED. Recent improvements in the measurement of the electron moment[1] and of the fine-structure constant[2] reveal an apparent discrepancy of 0.33(14) ppm between QED theory and experiment for the anomalous electron moment.[3] We report here an improved measurement of the Lamb shift in hydrogen which is also in poor agreement with QED predictions. Should these discrepancies persist, they could be important clues to the approximations inherent in our present understanding of electromagnetic interactions.

In the measurement reported here, the separated–oscillatory-field technique[4,5] is used to narrow the Lamb-shift resonance below its natural width of 100 MHz. A beam of fast hydrogen atoms in the $2^2S_{1/2}(F=0)$ state is prepared by charge exchange from a fast proton beam and radiofrequency hyperfine-state selection techniques. The beam passes through two separated, coherent oscillatory fields and the surviving number of metastable atoms is monitored by observing the Lyman-α photons emitted in Stark-induced decay to the ground state. The fractional quenching of the metastable beam by the separated oscillatory fields is measured for relative phases of 0° and 180° between the two fields. When averaged, these two signals give a large broad signal ($\overline{Q}$) whose width is determined by the natural linewidth and the transit time through the rf plates. The difference of the two signals $[I = Q(0°) - Q(180°)]$ gives the interference signal, whose width is determined by the transit time between the two regions. Measurements are made in zero magnetic field and the resonance observed by changing the frequency of the applied rf field while keeping its amplitude constant.

Figure 1 shows a typical line profile for the $2^2S_{1/2}(F=0)-2^2P_{1/2}(F=1)$ transition. For each configuration line profiles are taken with (a) the direction of propagation of the rf field in the interaction region reversed, (b) the time order in which the beam passed through the interaction region reversed, and both (a) and (b). The average center for four such lines is free from shifts due to the Doppler effect and rf phase errors. The average of the four linescans is found to be very symmetric; the raw data shows no asymmetry larger than 0.1% of the peak-to-peak interference signal. Thus the line centers can be determined by the method of symmetric points. As a check for systematic effects, measurements are made in eight different experimental configurations which differed in beam velocity, plate separation, and plate geometry. Table I lists the eight configurations together with the sizes and widths of the interference signals.

Table II summarizes the raw experimental centers and the corrections applied to obtain the $2^2S_{1/2}(F=0)-2^2P_{1/2}(F=1)$ interval for each of the eight configurations. The error in the raw center is the larger of the internal error (inferred from signal-measurement statistics) and the external error (inferred from scatter of measured centers). The origin of the corrections is as follows:

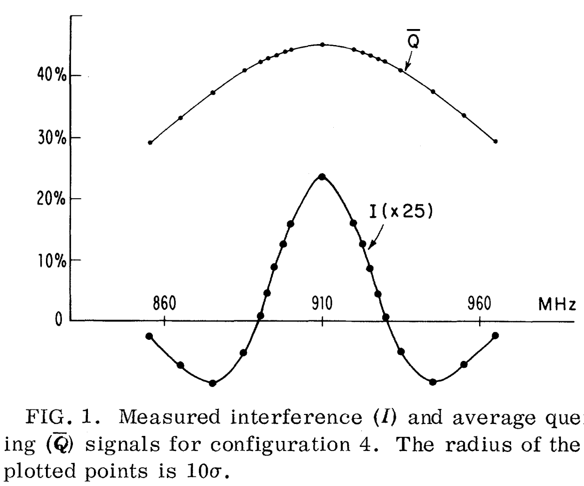

FIG. 1. Measured interference (I) and average quenching ($\overline{Q}$) signals for configuration 4. The radius of the plotted points is 10σ.

TABLE I. A summary of the configurations in which data were taken. One independent result requires four line profiles.

Configuration	Beam energy (keV)	Plate spacing (cm)	Peak-to-peak I signal (%)	Full width at half maximum (MHz)	Number of independent results
1	55.1(1.1)	2.34	6.08	45	5
2	55.1(1.1)	3.30[a]	3.65	41	8
3	55.1(1.1)	3.30	2.95	38	4
4	55.1(1.1)	4.30	1.35	32	4
5	55.1(1.1)	5.08	0.66	29	4
6	106.8(2.1)	5.08	1.82	35	8
7	106.8(2.1)	6.62	0.64	28	6
8	106.8(2.1)	7.60	0.37	25	2

[a]For configuration 2, the inner diameter of the cylindrical pipe surrounding the rf-field regions was increased from 3.81 to 5.08 cm.

(1) Time dilation. The resonance frequency should be measured in the moving atom's rest frame.

(2) Bloch-Siegert and rf Stark shifts. The shifts produced by the antiresonant $2^2S_{1/2}$-$2^2P_{1/2}$ coupling and nonresonant $2^2S_{1/2}$-$2^2P_{3/2}$ coupling. The net shift depends on plate spacing through a calculated geometrical factor.

(3) Plate coupling. The impedance of the rf plates depends slightly on whether they are driven with 0° or 180° relative phase.

(4) $F=1$. There are residual traces of the $2^2S_{1/2}(F=1)$ states.

(5) Incomplete $\overline{Q}$ subtraction. Systematic errors in the control of relative rf power between the 0° and 180° states may produce a small spurious signal.

(6) Off-axis distortion. Atoms traveling off-axis through the plates see a nonuniform rf-field polarity which leads to small shifts.

(7) rf-field slope. Laboratory calibration of the rf electric field strength within the plates indicates that, under experimental conditions, it varies by $\Delta E/E = -0.08(7)\%/(100\text{ MHz})$.

The result for each configuration, corrected for these seven effects, is shown in Table II in the row labeled "Subtotal". The associated error is the quadrature sum of random and systematic errors. Several other potential sources of systematic error have been studied and found to be negligible. These are overlapping resonances in high-n states detected through cascades, stray electric and magnetic fields, and coherent population of S and P states.

Evidence for the presence of residual systematic errors is given by a comparison of the centers determined in the eight configurations. Their χ^2 is 14.3 for 7 degrees of freedom and the centers correlate with the size of the interference signal. Further evidence is found by studying the symmetry of the measured resonance signals. Although theoretical studies indicate that after allowance for small systematic effects both $\overline{Q}$ and I should be symmetric about the same center, this was not found to be the case. Figure 2(a) shows the symmetric and antisymmetric parts of the $\overline{Q}$ signal for configuration 6, taken about the best center of the I signal for that configuration (909.818 MHz). The data have been corrected to remove expected asymmetries due to corrections 2, 4, and 6 in Table II. A small positive asymmetry remains, as was found in all configurations. Figure 2(b) shows the symmetric and antisymmetric parts of the interference signal for the same configuration about the same center frequency, again corrected for expected asymmetries. There is a small asymmetry in the region of the minimum of the signal.

All three of these effects can be accounted for by assuming that the rf electric field strength is increasing across the line. The size of the apparent increase may be determined independently from each effect, giving 0.88(30)%/(100 MHz), 0.30(15)%/(100 MHz), and 0.45(15)%/(100 MHz), respectively. Such an increase would seem to contradict field calibration measurements, which have an estimated precision of ± 0.07%/(100 MHz), due to uncertainty in National Bureau of Standards

TABLE II. A summary of the raw experimental centers and the corrections applied to obtain the $2^2S_{1/2}(F=0) - 2^2P_{1/2}(F=1)$ interval for each of the eight configurations.

Configuration	1	2	3	4	5	6	7	8	55 keV	107 keV
Raw Center (MHz)	909.930(8)	909.887(10)	909.893(6)	909.847(11)	909.844(18)	909.818(9)	909.807(11)	909.788(38)	909.891(4)	909.813(7)
Source of Error	External	External	External	Internal	Internal	Internal	External	External		
1) Time Dilation	0.053(2)	0.053(2)	0.053(2)	0.053(2)	0.053(2)	0.104(4)	0.104(4)	0.104(4)	0.053(2)	0.104(4)
2) Bloch-Siegert + rf Stark	-0.038(4)	-0.036(2)	-0.030(3)	-0.024(3)	-0.021(3)	-0.027(2)	-0.021(2)	-0.019(2)	-0.032(3)	-0.024(2)
3) Plate Coupling	-0.014(2)	-0.014(2)	-0.004(2)	-0.001(0)	-0.000(0)	-0.000(0)	-0.000(0)	-0.000(0)	-0.008(2)	-0.000(0)
4) F=1	-0.004(1)	-0.002(1)	0.000(0)	0.000(0)	0.000(0)	+0.001(0)	0.000(0)	0.000(0)	-0.001(0)	+0.001(0)
5) Incomplete $\bar{Q}$ Subtraction	0.000(2)	0.000(3)	0.000(3)	0.000(7)	0.000(13)	0.000(4)	0.000(8)	0.000(13)	0.000(4)	0.000(6)
6) Off-Axis Distortion	-0.006(4)	-0.003(2)	-0.003(2)	-0.003(2)	-0.003(2)	-0.003(2)	-0.002(1)	-0.002(1)	-0.004(2)	-0.003(2)
7) rf Field Slope	+0.004(3)	+0.003(2)	+0.001(1)	+0.001(1)	0.000(0)	-0.001(1)	0.000(0)	0.000(0)	+0.002(2)	-0.001(1)
Total 1-7	-0.005(7)	+0.001(5)	+0.017(6)	+0.026(8)	+0.029(14)	0.074(6)	+0.081(9)	+0.083(14)	+0.010(6)	+0.077(8)
Subtotal	909.925(11)	909.888(11)	909.910(9)	909.873(14)	909.873(23)	909.892(11)	909.888(14)	909.871(40)	909.901(7)	909.890(11)
8) Additional Field Slope	-0.025(10)	-0.018(7)	-0.009(3)	-0.006(2)	-0.002(1)	-0.005(2)	-0.002(1)	-0.002(1)	-0.014(5)	-0.004(2)
$\nu(2^2S_{\frac{1}{2}}(F=0) - 2^2P_{\frac{1}{2}}(F=1))$	909.900(15)	909.870(13)	909.901(9)	909.867(14)	909.871(23)	909.887(11)	909.886(14)	909.869(40)	909.887(9)	909.886(11)

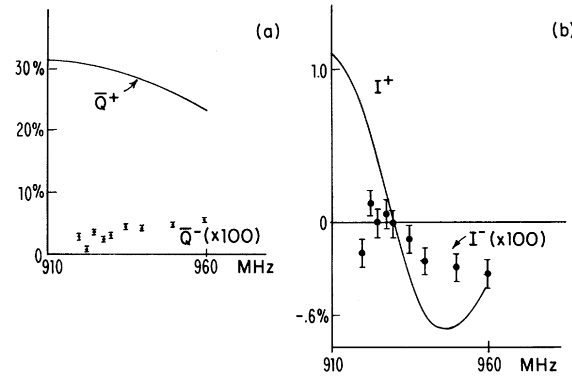

FIG. 2. (a) Symmetric and antisymmetric parts of $\bar{Q}$ for configuration 6 taken about 909.818 MHz, after correction for known systematic effects. (b) Symmetric and antisymmetric parts of I for configuration 6 taken about 909.818 MHz, after correction for know systematic effects.

standards for relative power measurement. It is also possible that some other effect mimics an error in the field calibration. Although our understanding of the physical origin of this effect is not complete, we choose to apply an *ad hoc* correction to the data based on an assumed additional increase of rf-field strength of +0.5(2)%/(100 MHz). This correction simultaneously brings the centers from all eight configurations into agreement and removes all asymmetries from both the $\bar{Q}$ and I signals.

Table II shows the correction applied for this additional field slope and the final determination of the $2^2S_{1/2}(F=0)$ to $2^2P_{1/2}(F=1)$ interval for each configuration. To compute the final result we combine the results from the 55-keV configurations (1–5) and 107-keV configurations (6–8) separately, weighting the individual results according to the inverse square of the total error shown in the line labeled "Subtotal." We assume that each systematic error is completely correlated between the different configurations, but that different systematic errors are mutually uncorrelated. The results for 55 and 107 keV are, respectively,

$$\nu(2^2S_{1/2}(F=0)-2^2P_{1/2}(F=1)) = 909.887(9) \text{ MHz},$$

$$\nu(2^2S_{1/2}(F=0)-2^2P_{1/2}(F=1)) = 909.886(11) \text{ MHz}.$$

The additional rf-field–slope correction contributes $-0.014(5)$ and $-0.004(2)$ MHz to the results at 55 and 107 keV, respectively.

A straight average of these results gives

$$\nu(2^2S_{1/2}(F=0) - 2^2P_{1/2}(F=1)) = 909.887(9) \text{ MHz},$$

with a random error of ± 0.004 MHz and a systematic error of ± 0.008 MHz. Correcting for the known hyperfine structure of the $2^2S_{1/2}$ and $2^2P_{1/2}$ states, the Lamb-shift interval is found to be

$$\mathcal{S}(\mathrm{H}, n=2) = 909.887(9) + 147.958\ \mathrm{MHz}$$
$$= 1057.845(9)\ \mathrm{MHz}.$$

This result is in good agreement with previous measurements of Lamb *et al.* [1057.77(6) MHz][6,7] and Robiscoe *et al.* [1057.90(6) MHz],[7,8] and with the more recent measurement of Newton, Andrews, and Unsworth [1057.862(20) MHz].[9] The disagreement with our own preliminary result [1057.892(20) MHz][5] can be accounted for by statistics and by systematic corrections 3 and 8 in Table II which were unknown to us at that time.

The predictions of QED for the Lamb-shift interval have been evaluated most precisely by Erickson[10] and Mohr[11]; when modified to reflect recent redeterminations of the proton rms charge radius [$r_p = 0.862(12)$ fm],[12] their results are, respectively,

$$\mathcal{S}(n=2) = 1057.930(10),$$
$$\mathcal{S}_{\mathrm{theor}} - \mathcal{S}_{\mathrm{expt}} = 0.085(13);$$
$$\mathcal{S}(n=2) = 1057.884(13),$$
$$\mathcal{S}_{\mathrm{theor}} - \mathcal{S}_{\mathrm{expt}} = 0.039(16).$$

Neither result is in good agreement with experiment. Further improvement in the experimental precision to the level of ± 0.001 MHz appears feasible with the technique used here.

We would like to acknowledge the support of the National Science Foundation through NSF Grant No. 78-09657.

[1]R. S. Van Dyck, Jr., P. B. Schwinberg, and H. G. Dehmelt, Bull. Am. Phys. Soc. 24, 758 (1979), and Phys. Rev. Lett. 38, 310 (1977).

[2]E. R. Williams and P. T. Olsen, Phys. Rev. Lett. 42, 1575 (1979).

[3]T. Kinoshita, in *New Frontiers in High Energy Physics—Studies in the Natural Sciences, Sanibel Island*, edited by A. Perlmutter and L. F. Scott (Plenum, New York, 1978), Vol. 14, p. 127.

[4]N. F. Ramsey, *Molecular Beams* (Oxford Univ. Press, London, 1956), p. 124.

[5]S. R. Lundeen and F. M. Pipkin, Phys. Rev. Lett. 34, 1368 (1975).

[6]S. Triebwasser, E. S. Dayhoff, and W. E. Lamb, Jr., Phys. Rev. 89, 98 (1953).

[7]B. N. Taylor, W. H. Parker, and D. N. Langenberg, Rev. Mod. Phys. 41, 375 (1969).

[8]R. T. Robiscow and T. W. Shyn, Phys. Rev. Lett. 24, 559 (1970).

[9]G. Newton, D. A. Andrews, and P. J. Unsworth, Phil. Trans. Roy. Soc. London 290, 373 (1979).

[10]G. W. Erickson, Phys. Rev. Lett. 27, 780 (1971).

[11]P. J. Mohr, Phys. Rev. Lett. 34, 1050 (1975).

[12]G. G. Simon, F. Borkowski, Ch. Schmitt, and V. W. Walther, Z. Naturforsch. 35A, 1 (1980).